

## Superconducting Joints Using Bi-added PbSn Solders

Ryo Matsumoto<sup>1,2</sup> \*, Hirotsugu Iwata<sup>1,2</sup>, Aichi Yamashita<sup>1,2</sup>, Hiroshi Hara<sup>1,2</sup>, Gen Nishijima<sup>1</sup>, Masashi Tanaka<sup>1,3</sup>, Hiroyuki Takeya<sup>1</sup>, and Yoshihiko Takano<sup>1,2</sup>

<sup>1</sup>*National Institute for Materials Science, 1-2-1 Sengen, Tsukuba, Ibaraki 305-0047, Japan*

<sup>2</sup>*Graduate School of Pure and Applied Sciences, University of Tsukuba, 1-1-1 Tennodai, Tsukuba, Ibaraki 305-8577, Japan*

<sup>3</sup>*Graduate School of Engineering, Kyushu Institute of Technology, 1-1 Sensui-cho, Tobata, Kitakyushu 804-8550, Japan*

E-mail: MATSUMOTO.Ryo@nims.go.jp

Superconducting joints between NbTi and Bi<sub>2</sub>Sr<sub>2</sub>Ca<sub>2</sub>Cu<sub>3</sub>O<sub>10</sub> superconducting wires were successfully fabricated using Bi-added PbSn solders with *in-situ* sheath-dissolution technique without a removing process of sheath materials. A back scattered electron image and an energy-dispersive X-ray spectroscopy analysis of the cross sectional plane of the joints showed that the joints using Bi-added PbSn solder have a homogeneous morphology with tiny non-superconducting islands. The superconducting joints show high critical currents above 200 A in self-field and 50 A under the applied magnetic field of 5 kOe.

Recently, a nuclear magnetic resonance (NMR) spectrometer operated at 1020 MHz, corresponding to a magnetic field of 24 T, has been developed<sup>1, 2)</sup>. It was demonstrated that the quality of the 2-dimensional solid-state NMR spectrum of a membrane protein by 1020 MHz NMR was considerably better than that obtained by a conventional 700 MHz NMR magnet<sup>3)</sup>. The superconducting magnet in the NMR apparatus consists of outer coils using low-transition temperature ( $T_c$ ) superconductors (LTS) of NbTi and Nb<sub>3</sub>Sn, and an innermost coil using high- $T_c$  superconductor (HTS) of Bi<sub>2</sub>Sr<sub>2</sub>Ca<sub>2</sub>Cu<sub>3</sub>O<sub>10</sub> (Bi2223)<sup>4)</sup>. The LTS outer coils and the HTS innermost coil are connected in series.

Joints in a commercially available NMR superconducting magnet are fabricated using a superconducting joint technique<sup>5)</sup>. The superconducting joints make it possible to operate the NMR magnet in a persistent-current mode, which can drive the magnet without external power-supply. However, the 1020 MHz NMR magnet has been designed and operated in a power-supply-driven mode<sup>6)</sup> since the superconducting joint technique has not been developed sufficiently for the joint between LTS and Bi2223. To realize the persistent-current mode operation of the 1020 MHz NMR magnet, superconducting joints of LTS-Bi2223 are necessary.

A solder dip method using Pb-based alloy is a famous technique to obtain the superconducting joint between LTS wires<sup>7-11)</sup>. Literatures have been published that reported ultralow resistance values, *e.g.*, less than  $10^{-11} \Omega$  in 1.5 T at 4.2 K<sup>8)</sup> and less than  $10^{-13} \Omega$  for a NbTi-NbTi joint in 0.7–1.0 T at 4.2 K<sup>11)</sup>. However, the superconducting joints between LTS and Bi2223 wires have not been realized yet.

In this study, we have successfully demonstrated the superconducting joints between NbTi and Bi2223 superconducting wires by an *in-situ* sheath-dissolution method using Bi-added PbSn solders. The microstructure and compositional ratio of the joints were investigated by energy dispersive X-ray spectroscopy (EDX) and back scattered electron (BSE) images using a scanning electron microscope (SEM). The  $T_c$  and critical current ( $I_c$ ) of the joints were measured under various magnetic fields.

Joint samples were fabricated by using a NbTi and a Bi2223 wires. The NbTi wire is standard reference material SRM 1457, available from the National Institute of Standards and Technology (NIST)<sup>12)</sup>. It is a multifilamentary wire of 0.51 mm diameter, consists of 180 NbTi filaments in a Cu matrix<sup>13)</sup>. Typical  $T_c$  is 8.9 K in 2 T and  $I_c$  is 290 A at 4.2 K in 2

T<sup>12</sup>). The Bi2223 wire is DI-BSCCO type H, purchased from Sumitomo Electric Industries. It is a  $4.4 \times 0.22 \text{ mm}^2$  tape-shaped multifilamentary wire with Ag sheath. The  $T_c$  is 110 K and the  $I_c$  is 206 A at 77.3 K in self-field.

The non-superconducting sheath materials of Cu and Ag are generally removed from the superconducting wire before the jointing process. An acid etching treatment is often used to remove the sheath materials from superconducting wires. However, the etching treatment sometimes damages the superconducting filaments, and often deteriorates the superconducting properties. We therefore developed the *in-situ* sheath-dissolution method to remove the sheath materials from superconducting filaments without acid damage. In this method, superconducting wires are inserted into molten solder with their sheath materials. When the sheath materials are dissolved into the solder, the superconducting wires are directly contacted to the solder. Since the contacted solder shows superconductivity, the two wires are connected by superconductors, namely it becomes superconducting joints.

Then the superconducting joints were fabricated using the PbSn solders by the *in-situ* sheath-dissolution method. The superconducting solders of PbSn eutectics with several different Sn content ratios  $x$  as  $\text{Pb}_{1-x}\text{Sn}_x$  were synthesized at 400 °C for 10 hours in an evacuated quartz tube. A quartz container was filled with the obtained PbSn solder. When the solder was completely melted in a furnace at 400 °C for 10 minutes, the NbTi wire with the Cu-sheath and the Bi2223 wire with the Ag-sheath were dipped into the solder as shown in Fig. 1(a). The lengths of superconducting wires were ~30 mm. The solder width and the dip lengths were ~5 mm and ~10 mm, respectively. After annealing at 400 °C for 4 hours, the sample was cooled down to room temperature in the furnace, and then, the NbTi and the Bi2223 wires were connected by the PbSn solder.

The microstructures of the superconducting joints were observed using BSE mode of a SEM (JEOL JSM-6010LA) operated at an acceleration voltage of 20 kV, at a cross-sectional region displayed by red line in Fig. 1(a). Figure 1(b) shows a BSE image of a polished cross-section around the joint of NbTi and Bi2223 wires using  $\text{Pb}_{0.5}\text{Sn}_{0.5}$  solder. There were two phases of a dark region and a bright region in the solder part. The Cu and Ag sheath materials were dissolved into the dark region of the solder matrix, and then the surface of superconducting filaments of NbTi and Bi2223 appeared to be totally covered

by the superconducting PbSn eutectics of the bright region with different Sn content ratios. Therefore, the *in-situ* sheath-dissolution method seems to be effective to connect superconducting wires without the removing process of sheath materials. The sheath materials of Cu and Ag sometimes remained around superconducting wires when the amount of Sn was decreased. It indicates that the sufficient amount of Sn in the solder is necessary to remove the sheath materials from superconducting wires completely. On the other hand, the bright region in the solder part tended to decrease with increase of nominal Sn contents as is observed in Fig. 1(c). A superconducting joint using  $\text{Pb}_{0.7}\text{Sn}_{0.3}$  would be expected to have the best  $I_c$  value among them, reflecting its homogeneous morphology.

Transport properties of the joints were measured by a four-probe method using terminals of  $I^+$ ,  $I^-$ ,  $V^+$  and  $V^-$  as shown in Fig. 1(a). Figure 2(a) shows the temperature dependence of resistance for the joint using  $\text{Pb}_{0.7}\text{Sn}_{0.3}$ . The superconducting transitions with onset temperature were observed at around 9.7 K and 7.7 K, corresponding to  $T_c$  of NbTi wire and PbSn alloy, respectively. The resistance dropped to zero at 7.4 K. The transition width of PbSn alloy was slightly broader than the transition of NbTi, probably due to the inhomogeneity of Pb-Sn ratio. Figure 2(b) shows the current-voltage ( $I$ - $V$ ) characteristics of the joint using  $\text{Pb}_{0.7}\text{Sn}_{0.3}$  and pure Pb at 4.2 K (liquid He bath) under self-field. The broken line in the figure is the criterion for the  $I_c$  of 1  $\mu\text{V}$ . The output limit of the current source was 200 A. As shown in the  $I$ - $V$  curve of the joint using  $\text{Pb}_{0.7}\text{Sn}_{0.3}$ , the voltage did not appear within the criterion until 115 A, indicating that the  $I_c$  of PbSn solder joints was drastically enhanced compare to the joint with only pure Pb. The estimated resistance for  $\text{Pb}_{0.7}\text{Sn}_{0.3}$  joint was  $9 \times 10^{-9} \Omega$ , which was calculated from the voltage divided by  $I_c$  of 115 A at criterion of 1  $\mu\text{V}$ . As a further evaluation, the resistance should be derived from the current decay in a loop circuit with the joint to obtain actual joint resistance.

Figure 3 shows  $I_c$  of the joint under various applied magnetic fields at 4.2 K as a function of Sn contents  $x$  in  $\text{Pb}_{1-x}\text{Sn}_x$ . The highest  $I_c$  was obtained around the Sn contents of  $x = 0.3$  in the case of the self-field measurement. This result means that the compositional ratio of  $\text{Pb}_{0.7}\text{Sn}_{0.3}$  was an optimum value from the view point of  $I_c$  value in self-field. The  $I_c$  tended to decrease with increase of Sn contents  $x$ . On the other hand, the joint at  $\text{Pb}_{0.5}\text{Sn}_{0.5}$  shows relatively lower  $I_c$ , even though the corresponding alloy has higher  $T_c$  and critical field compare to the other ratios<sup>14)</sup>. The lower  $I_c$  of the joint with  $\text{Pb}_{0.5}\text{Sn}_{0.5}$  was repeatedly

observed in the other measurement using different sample batches, although the reason is unclear.

Against increase of magnetic field, all joints immediately decreased their  $I_c$  values. The rapid  $I_c$  drop is attributed to the low critical field such as a type I superconductor in the component of the joint, *i.e.*, PbSn solder<sup>14</sup>). These joints are not applicable for practical use, because joints in a practical superconducting magnet are usually exposed to magnetic field. Hence, it is necessary to enhance the  $I_c$  in magnetic fields. Then we added Bi to the optimum  $\text{Pb}_{0.7}\text{Sn}_{0.3}$  solder joint, evoked from an idea of the higher critical field in PbBi of type II superconductor<sup>15</sup>).

The Bi-added PbSn solders were synthesized with different Bi amount  $y$  in  $(\text{Pb}_{0.7}\text{Sn}_{0.3})_{1-y}\text{Bi}_y$ ,  $y = 0-0.95$ . The mixtures of the starting material of Pb, Sn, and Bi were sealed into an evacuated quartz tube and heated at 400 °C for 10 hours. The annealed samples were cooled down to room temperature in a furnace. The joints between NbTi and Bi2223 wires were fabricated by the *in-situ* sheath-dissolution method using obtained Bi-added PbSn solders.

Figure 4 shows BSE images of polished cross-section of the solder part in the superconducting joints using (a)  $\text{Pb}_{0.7}\text{Sn}_{0.3}$  solder without Bi addition as a reference, and (b)  $(\text{Pb}_{0.7}\text{Sn}_{0.3})_{0.7}\text{Bi}_{0.3}$  solder. It was found that the microstructure of the joint using  $\text{Pb}_{0.7}\text{Sn}_{0.3}$  contained two distinct contrasted regions on the morphology from the BSE image. The major and the minor phases in the matrix were confirmed to be  $\text{Pb}_{0.74}\text{Sn}_{0.26}$  and  $\text{Sn}_{0.24}\text{Ag}_{0.76}$  by EDX analysis, respectively. Although PbSn part is superconductor, the SnAg island part is not superconductor at liquid He temperature<sup>16, 17</sup>). This minor phase leads to suppress the total  $I_c$  of the solder due to a restricted superconducting current path. On the other hand,  $(\text{Pb}_{0.7}\text{Sn}_{0.3})_{0.7}\text{Bi}_{0.3}$  solder showed relatively homogeneous morphology as shown in Fig. 4(b). There are two phases in the solder:  $\text{Pb}_{0.63}\text{Sn}_{0.1}\text{Bi}_{0.27}$  as a major phase and small  $\text{Sn}_{0.95}\text{Bi}_{0.05}$  island as a minor phase. The minor phase of  $\text{Sn}_{0.95}\text{Bi}_{0.05}$  does not show superconductivity at liquid He temperature<sup>18</sup>). The non-superconducting area in the Bi-added solder was quite less than that in the  $\text{Pb}_{0.7}\text{Sn}_{0.3}$  solder.

Figure 5 shows temperature dependence of resistance from 5 K to 10 K of  $\text{Pb}_{0.7}\text{Sn}_{0.3}$  and  $(\text{Pb}_{0.7}\text{Sn}_{0.3})_{0.7}\text{Bi}_{0.3}$  solders. The resistances of the solders are normalized at 10 K. The temperature dependences of resistance for the  $\text{Pb}_{0.7}\text{Sn}_{0.3}$  and the  $(\text{Pb}_{0.7}\text{Sn}_{0.3})_{0.7}\text{Bi}_{0.3}$  solders

show sharp superconducting transitions at around 7.5 K and 8.2 K, respectively. It was found that the Bi-addition enhanced the zero-resistivity temperature of the PbSn solder.

The  $I_c$  values of the joint were measured under various magnetic fields at 4.2 K. Figure 6 shows  $I_c$  of the joint under various applied magnetic fields up to 5 kOe as a function of Bi contents  $y$  in  $(\text{Pb}_{0.7}\text{Sn}_{0.3})_{1-y}\text{Bi}_y$ . The Bi added  $\text{Pb}_{0.7}\text{Sn}_{0.3}$  solder drastically enhanced the  $I_c$  of the NbTi-Bi2223 joint under magnetic fields. The  $I_c$  of the joint with  $y = 0.1$  to  $0.7$  were above 200 A in self-field. In particular, the  $I_c$  values were above 50 A even under the magnetic field of 5 kOe in a region between  $y = 0.3$  and  $0.4$ . However, the excessive addition of  $y = 0.8$  to  $0.95$  suppressed  $I_c$ , probably due to the precipitation of a Bi metal that is not superconductor at 4.2 K.

These results show the Bi-addition is effective to enhance the  $I_c$  in magnetic fields. This  $I_c$  enhancement can be explained by the homogeneous microstructure in the Bi-added  $\text{Pb}_{0.7}\text{Sn}_{0.3}$  solder as shown in Fig. 4 (b). The BSE image gives us the other expectation for the reason of  $I_c$  enhancement. There are  $\text{Sn}_{0.95}\text{Bi}_{0.05}$  islands with a size of a few micrometers and widely distributed islands less than submicron with the same contrast in  $\text{Sn}_{0.95}\text{Bi}_{0.05}$ . The non-superconducting islands could be acted as flux pinning sites<sup>5, 19)</sup>, which enhances  $I_c$  under magnetic fields. On the other hand, some large  $\text{Sn}_{0.95}\text{Bi}_{0.05}$  islands also distribute in the solder as shown in Fig. 4(b). Further efforts to obtain more minutely dispersed  $\text{Sn}_{0.95}\text{Bi}_{0.05}$  islands that play a role of effective pinning sites are needed to enhance in-field property of the joints.

In summary, superconducting joints between NbTi and Bi2223 wires were successfully fabricated by the developed *in-situ* sheath-dissolution method using Bi-added PbSn superconducting solder. The cross-section of the joint using  $(\text{Pb}_{0.7}\text{Sn}_{0.3})_{0.7}\text{Bi}_{0.3}$  solder shows distributed non-superconducting islands in contrast to that using  $\text{Pb}_{0.7}\text{Sn}_{0.3}$  solder. The homogeneous structure enhanced the joint  $I_c$  above 200 A, beyond the measurement limit of this study in self-field and 50 A under magnetic field of 5 kOe at 4.2 K. Further joint resistance evaluation with a loop circuit is necessary in the future. The evolution of this joint technology would open a possibility to realize not only HTS/LTS magnet with the persistent current operation mode but also the other products of large scale superconducting applications.

### **Acknowledgments**

The authors gratefully acknowledge the help for polish of the sample surface by Mr. K. Nakazato (NIMS Materials Manufacturing and Engineering Station).

This work was partly supported by JST CREST, Japan, and JSPS KAKENHI Grant Number JP17J05926.

## References

- 1) K. Hashi, S. Ohki, S. Matsumoto, G. Nishijima, A. Goto, K. Deguchi, K. Yamada, T. Noguchi, S. Sakai, M. Takahashi, Y. Yanagisawa, S. Iguchi, T. Yamazaki, H. Maeda, R. Tanaka, T. Nemoto, H. Suematsu, T. Miki, K. Saito, and T. Shimizu, *J. Magn. Reson.* **256**, 30 (2015).
- 2) G. Nishijima, S. Matsumoto, K. Hashi, S. Ohki, A. Goto, T. Noguchi, S. Iguchi, Y. Yanagisawa, M. Takahashi, H. Maeda, T. Miki, K. Saito, R. Tanaka, and T. Shimizu, *IEEE Trans. Appl. Supercond.* **26**, 4303007 (2016).
- 3) K. Hashi, K. Deguchi, T. Yamazaki, S. Ohki, S. Matsumoto, G. Nishijima, A. Goto, K. Yamada, T. Noguchi, S. Sakai, M. Takahashi, Y. Yanagisawa, S. Iguchi, H. Maeda, R. Tanaka, T. Nemoto, H. Suematsu, J. To, J. Torres, K. Pervushin, and T. Shimizu, *Chem. Lett* **45**, 209 (2016).
- 4) T. Kiyoshi, S. Choi, S. Matsumoto, K. Zaitso, T. Hase, T. Miyazaki, M. Hamada, M. Hosono, and H. Maeda, *IEEE Trans. Appl. Supercond.* **21**, 2110 (2011).
- 5) G. D. Brittles, T. Mousavi, C. R. M. Grovenor, C. Aksoy, and S. C. Speller, *Supercond. Sci. Technol.* **28**, 093001 (2015).
- 6) G. Nishijima, S. Matsumoto, K. Hashi, S. Ohki, A. Goto, T. Noguchi, S. Sakai, and T. Shimizu *IEEE Trans. Appl. Supercond.* **26**, 4303304 (2016).
- 7) R. F. Thornton, U.S. Patent 4,584,547 (1986).
- 8) C. A. Swenson, and W. D. Markiewicz, *IEEE Trans. Appl. Supercond.* **9**, 185 (1999).
- 9) T. Fukuzaki, H. Maeda, S. Matsumoto, S. Nimori, S. Yokoyama, and T. Kiyoshi, *IEEE Trans. Appl. Supercond.* **16**, 1547 (2006).
- 10) J. Cheng, J. Liu, Z. Ni, C. Cui, S. Chen, S. Song, L. Li, Y. Dai, and Q. Wang, *IEEE Trans. Appl. Supercond.* **22**, 4300205 (2012).
- 11) M. Kodama, K. Okamoto, Y. Koga, T. Yamamoto, and H. Watanabe, *Supercond. Sci. Technol.* **28**, 045019 (2015).
- 12) L. F. Goodrich, D. F. Vecchia, E. S. Pittman, J. W. Ekin, and A. F. Clark, *NBS Special publication* **260-91** (1984).
- 13) VAMAS Technical Working Party for Superconducting Materials, *Cryogenics* **35**, S65 (1995).
- 14) W. H. Warren, and W. G. Bader, *Res. Rev. Sci. Instrum.* **40**, 180 (1969).

- 15) J. E. Evetts, and J. M. A. Wade, *J. Phys. Chem. Solids* **31**, 973 (1970).
- 16) D. C. Hamilton, Ch. J. Raub, B. T. Matthias, E. Corenzwit, and G. W. Hull, *J. Phys. Chem. Solids* **26**, 665 (1965).
- 17) H. L. Luo, and K. Andres, *Phys. Rev. B* **1**, 3002 (1970).
- 18) W. F. Love, *Phys. Rev.* **92**, 238 (1953).
- 19) J. D. Livingston, *J. Appl. Phys.* **38**, 2408 (1967).

## Figure Captions

**Fig. 1.** (a) Schematic image of the superconducting joint, (b) BSE image of polished cross-section around the superconducting joint of NbTi and Bi2223 wires using PbSn solder, (c) Enlargements of the BSE image around the solder part for the joints using  $\text{Pb}_{0.7}\text{Sn}_{0.3}$ ,  $\text{Pb}_{0.5}\text{Sn}_{0.5}$  and  $\text{Pb}_{0.36}\text{Sn}_{0.64}$  solders.

**Fig. 2.** Transport properties of (a) temperature dependence of resistance for the joint using  $\text{Pb}_{0.7}\text{Sn}_{0.3}$  and (b) current-voltage curves of the joint using  $\text{Pb}_{0.7}\text{Sn}_{0.3}$  and pure Pb at 4.2 K. The broken line in the figure is the criterion for the  $I_c$  of 1  $\mu\text{V}$ . Both measurements were conducted in self-field.

**Fig. 3.** Critical current of the joint under various applied magnetic fields at 4.2 K as a function of Sn contents  $x$  in  $\text{Pb}_{1-x}\text{Sn}_x$ . Solid curves are guides for eyes.

**Fig. 4.** BSE images of polished cross-section of the solder part in the superconducting joints using (a)  $\text{Pb}_{0.7}\text{Sn}_{0.3}$  solder without Bi addition as a reference and (b)  $(\text{Pb}_{0.7}\text{Sn}_{0.3})_{0.7}\text{Bi}_{0.3}$  solder.

**Fig. 5.** Temperature dependence of resistance from 5 K to 10 K of  $\text{Pb}_{0.7}\text{Sn}_{0.3}$  and  $(\text{Pb}_{0.7}\text{Sn}_{0.3})_{0.7}\text{Bi}_{0.3}$  solders.

**Fig. 6.** Critical current of the joint under various applied magnetic fields at 4.2 K as a function of Bi contents  $y$  in  $(\text{Pb}_{0.7}\text{Sn}_{0.3})_{1-y}\text{Bi}_y$ . Solid curves are guides for eyes.

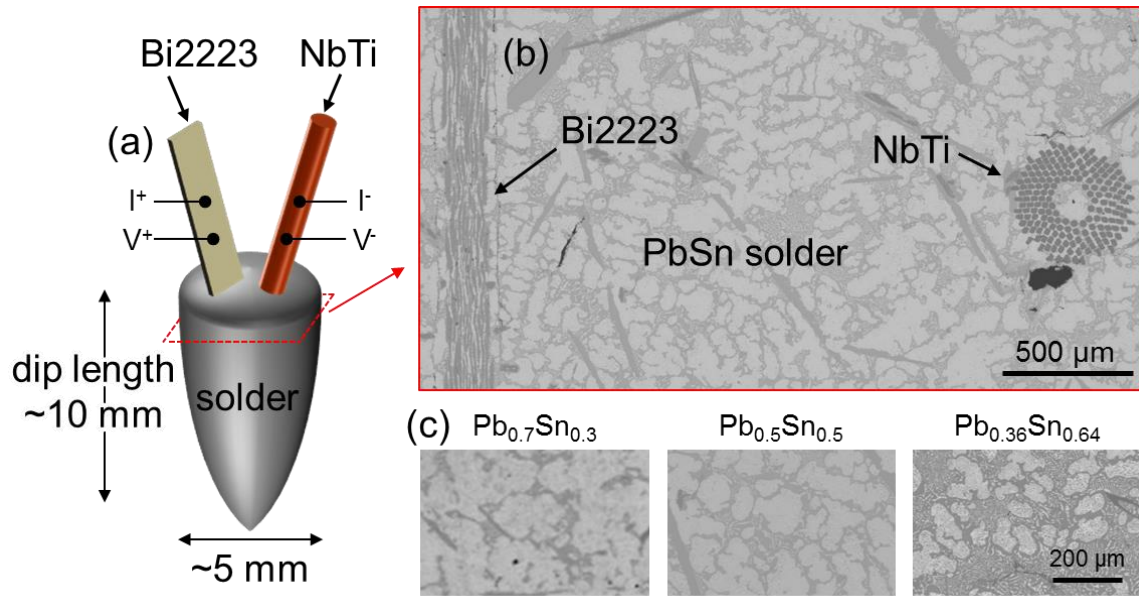


Fig.1.

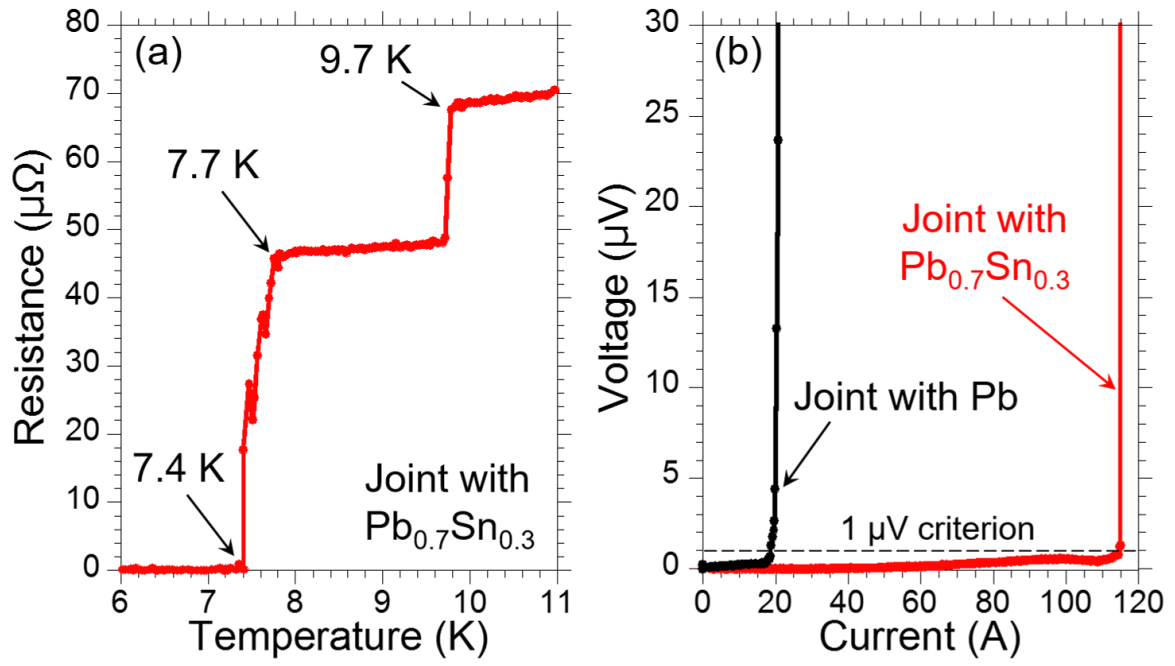


Fig. 2.

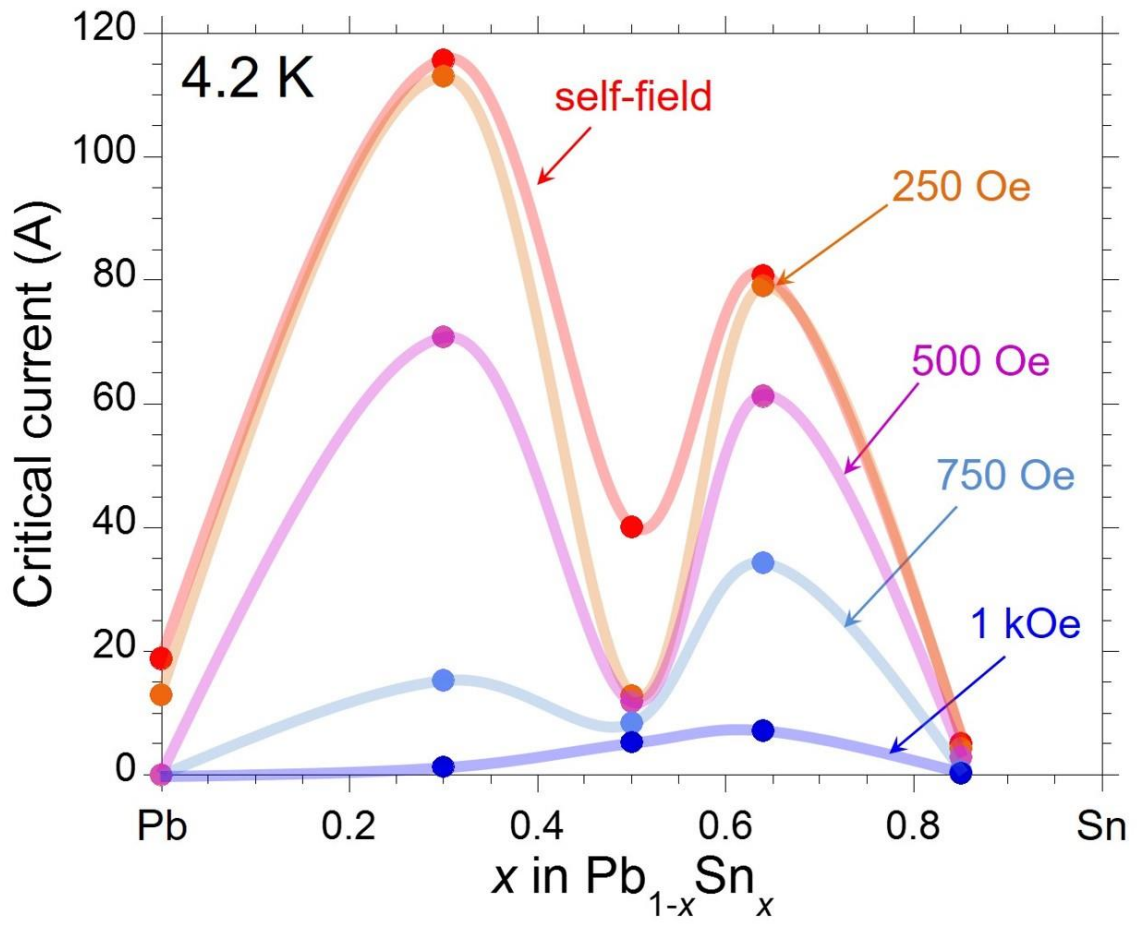


Fig. 3.

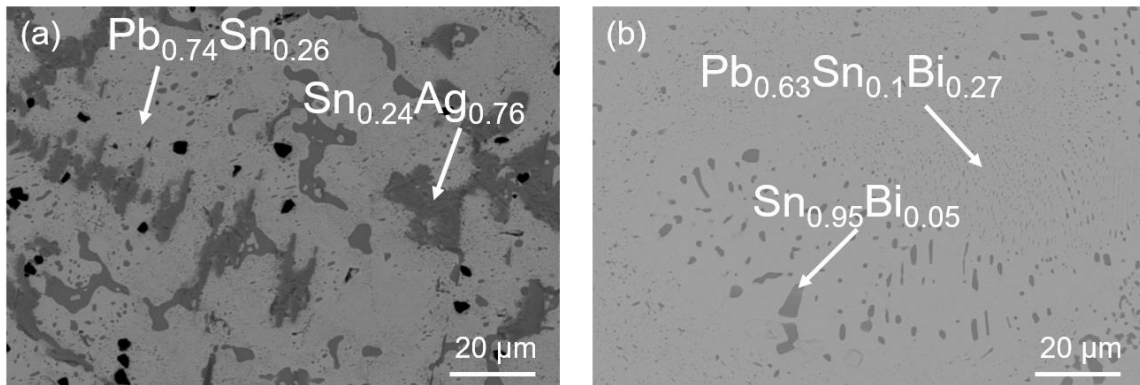


Fig. 4.

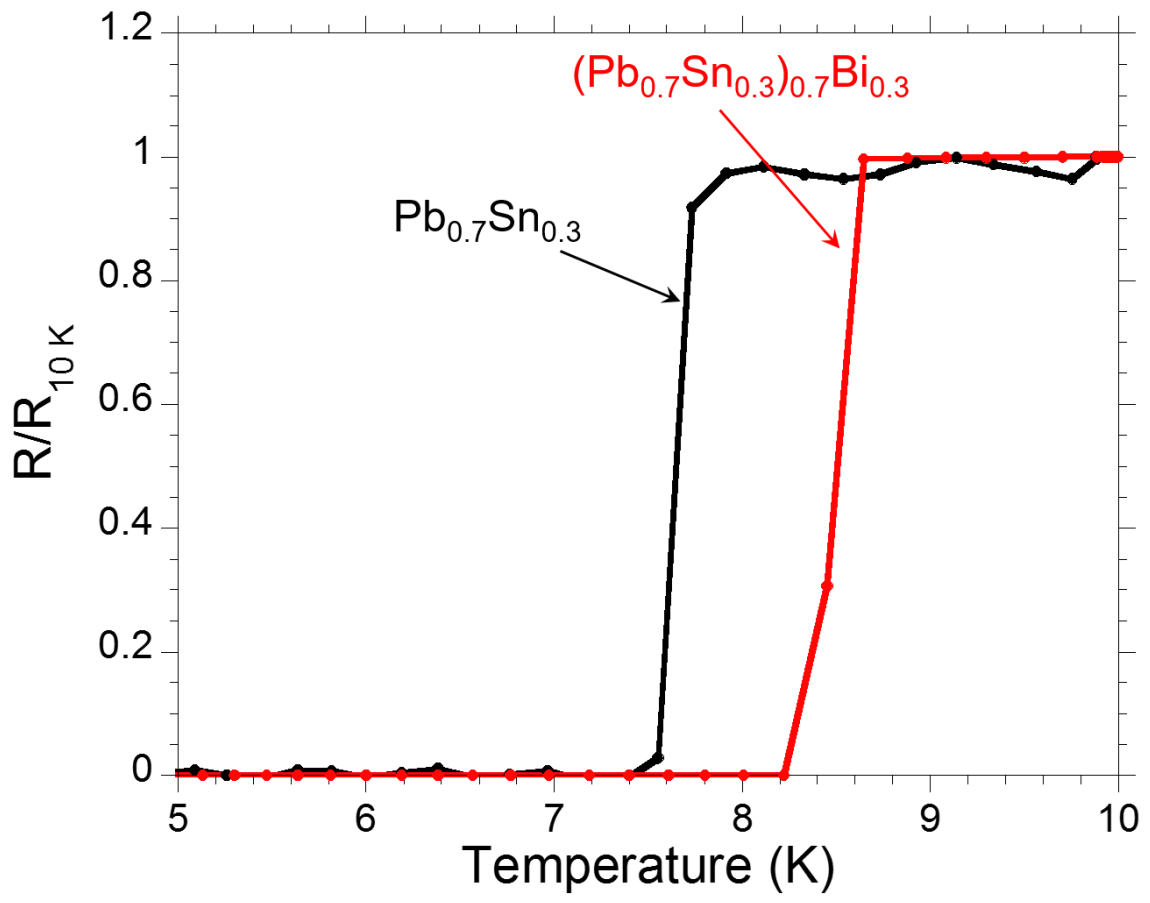


Fig. 5.

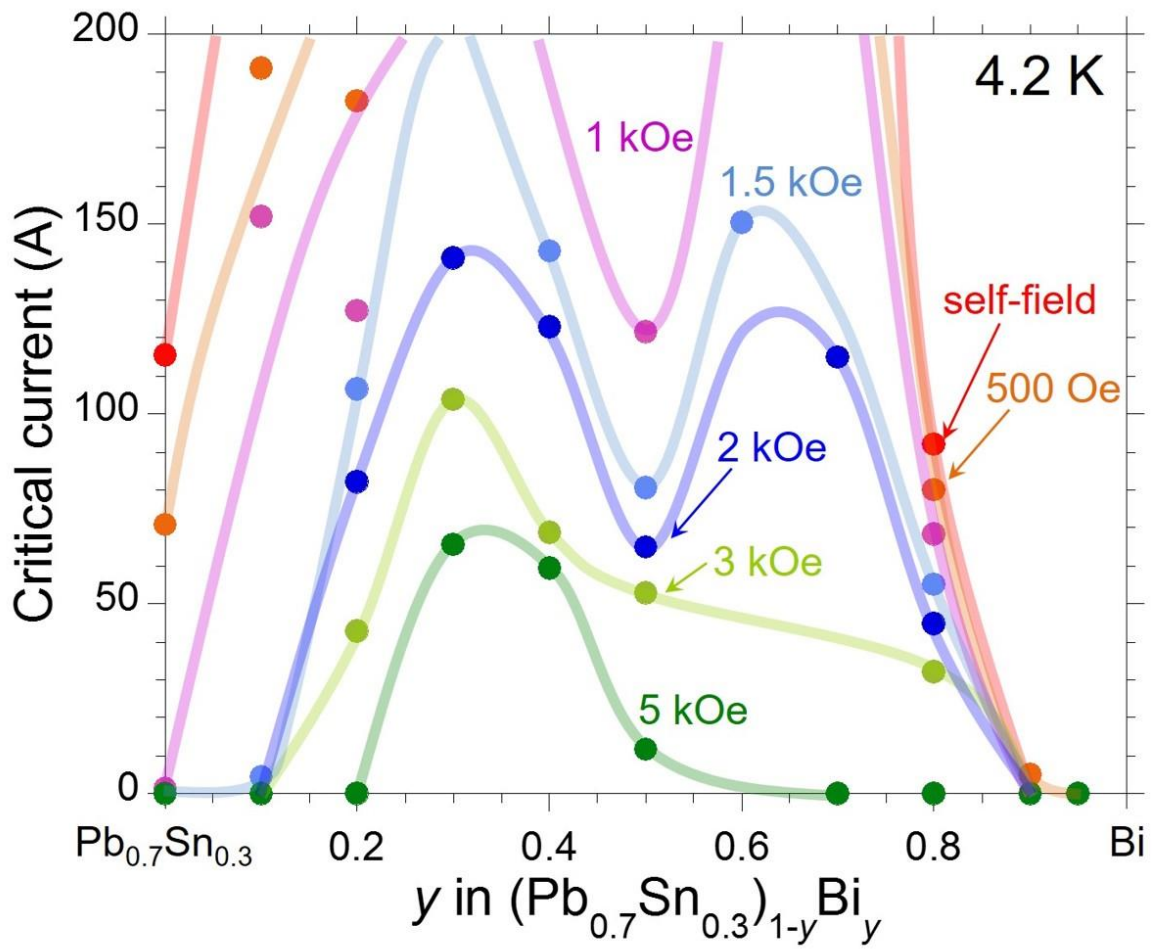


Fig. 6.